Microstructure and Properties of FeAlC-x(WC-Co) Composite Coating Prepared through Plasma Transfer Arc Cladding

Bai-Yang Chen , Bo Zhang , Daming Zhao , Peihu Gao * , Anton Naumov , Qi-bao Li , Fei Li , Zhong Yang , Yongchun Guo , Jian-Ping Li * , Bao-Long Wu , Jin-Yuan Gong , Jia-Wei Liu

Posted Date: 18 December 2023

doi: 10.20944/preprints202312.1334.v1

Keywords: plasma cladding; coating; compacted graphite cast iron; wear resistance

Article

Microstructure and Properties of FeAlC-x(WC-Co) Composite Coating Prepared through Plasma Transfer Arc Cladding

Bai-yang Chen [1,2], Bo Zhang [1], Da-ming Zhao [1], Pei-hu Gao [1,2]*, Anton Naumov [3], Qibao Li [1], Fei Li [1], Zhong Yang [1,2], Yong-Chun Guo [1,2], Jian-Ping Li [1,2]*, Bao-Long Wu [4], Jin-Yuan Gong [4] and Jia-Wei Liu [4]

1 School of Materials and Chemical Engineering, Xi'an Technological University, Xi'an 710021, Shaanxi, China; baiyang2578@163.com (B.-Y.C.); bozhang@163.com (B.Z.); zhaodaming@xacmkj.com (D.-M.Z.); liqibao@st.xatu.edu.cn (Q.-B. L); lifei814990635@163.com (F. L.); yz750925@163.com (Z.Y.); yc_guo@163.com (Y.-C.G.);
2 Shaanxi Province Engineering Research Centre of Aluminum/Magnesium Light Alloy and Composites, Xi'an 710021, Shaanxi, China
3 Lightweight Materials and Structures Laboratory, Institute of Mechanical Engineering, Materials and Transport, Peter the Great St. Petersburg Polytechnic University, St. Petersburg 195251, Russia; anton.naumov@spbstu.ru (A. N.)
4 Shaanxi North Dynamic Co., Ltd., Baoji 721300, Shaanxi, China; wubl@163.com (B.-L. W.); 1169154058@qq.com (J.-Y. G.); 172665561@qq.com (J.-W. L.)
* Correspondence: tigergaopei@163.com (P.-H.G.); Tel.: +86-29-83208080 (P.-H.G.); jpli@xatu.edu.cn (J.-P.L.); Tel.: +86-29-86173224 (J.-P.L.)

Abstract: Tungsten carbide (WC) was well known as a wear-resistant material. Iron-based powder was suitable for remanufacturing of cast iron engine parts. To improve the wear resistance of the remanufactured iron-based cast iron engine parts, WC-Co was introduced into iron-based powders to prepare composite coatings for cast iron engine components. In this work, FeAlC-x(WC-Co) composite coatings were prepared by plasma transfer arc on compacted graphite cast iron. The influences of WC-Co contents in the Fe-AlC-x(WC-Co) composite coatings on the microstructure and properties of the composite coatings were investigated. The composite coatings contained γ-Fe, α-Fe, WC and Fe_3W_3C mainly. The microhardness of FeAlC-x(WC-Co) composite coatings had the highest hardness of 814 HV0.2, the-lowest coefficient of 0.5 and the lest wear mass loss of 1.3mg when the weight content of WC-Co in the composite coating was 20wt%. As compared with the FeAlC coating, FeAlC-x(WC-Co) composite coating achieved the effect of reducing friction and wear resistance simultaneously, which resulted from the self-lubricating effect of graphite and high wear-resistance of carbides in the claddings.

Keywords: plasma cladding; coating; compacted graphite cast iron; wear resistance

1. Introduction

Compared with the traditional grey cast iron, compacted cast iron has gradually become the primary cast iron material for engine components because of its excellent mechanical and physical properties for the worm-shaped graphite [1-3]. In long-term serving, compacted graphite cast iron will undergo wear on its surface inevitably, which will affect the safe use in the equipment or machines [4]. The wear dimension of engine parts can be recovered through remanufacturing [5]. Meanwhile, wear resistant material can be introduced to enhance the surface wear resistance of newly manufactured or remanufactured engine parts.

In order to repair the failed parts, different methods have been used to repair or remanufacture cast iron engine parts. Thermal spraying technologies, such as plasma spraying and high velocity oxy-fuel (HVOF) spraying [6-9], were often used to recover wear dimensions of engine parts. While, bonding between coating and cast iron substrate was mainly mechanical adhesion which made the coatings hard to service in heavy load. Cold spray, depending on the plastic deformation of sprayed

 doi:10.20944/preprints202312.1334.v1

powders, could achieve compact coatings, while its adhesion between coating and substrate was mainly mechanical [10]. Additional heat treatments were needed to increase the strengthen of the combination between the coating and substrate. Laser cladding was an effective method to prepare coatings with metallurgical combination between coating and substrate [11-13]. Plasma transferred arc (PTA) cladding was another surfacing technology, which could form metallurgical combination between coating and substrate with less cost as compared to laser cladding method [14-17]. Therefore, PTA was preferred to prepare coatings on cast iron or remanufacture cast iron parts with well adhesions.

To improve the wear resistance of cast iron furtherly, hard phases, such as WC, TiC, Al_2O_3 and so on, were introduced into metals in the surface materials, which formed metal matrix composite (MMC) coatings. MMC coatings had good comprehensive properties with hard particles embedded in a tough metal matrix or binder [19-20]. Tungsten carbide (WC) was well known as a wear-resistant material with a good combination of hardness, toughness as well as wear resistance. Among metal-based reinforcements, WC particles is recognized to be one of the most commonly used hard-phase which combines lows thermal expansion coefficient, high hardness and good wettability [21]. Xie et al[20]. designed stellite Ni-based alloy powder mixed with Ni-coated WC to deposit coatings on AISI 1054 steel through PTA. Metallurgical bond formed between the coating and AISI 1054 steel substrate. Meanwhile, the microhardness increased from 400HV to 600HV. Peng et al [22] prepared FeCoCrNi high-entropy alloy/WC composite coating on steels through PTA. When WC content was higher than 60%, the coatings consisted of WC, FCC phase of HEA, Fe_3W_3C phase and Cr-rich secondary solid solution phase. The carbides improved the hardness and wear resistance of the coating. K.Y. Shi et al [23] employed PTA to deposit TiC-W-Cr powders on grey cast iron. The cladding zone consisted of primary austenite, martensite, carbide and un-melted TiC particles. Within the TiC-W-Cr cladding layer, the fatigue crack growth rate decreased at low stress strength.

Although the typical materials commonly used in the preparation of metal matrix composite (MMC) coatings are cobalt-based, nickel-based, high-entropy alloys, and iron-based alloy powders [24-25], the most widely used t is still iron-based alloy at present, due to their low cost and high performance. Since most of the workpiece materials are iron-based materials, it is more appropriate to use iron-based powder in repairing failed iron workpieces. Meanwhile, the use of iron-based alloy powders with the same or similar chemical composition to the substrate material would ensure better metallurgical bonding interface and similar properties. Xiao [26] et al. prepared the Fe-WC composite coatings with 0~60 wt.% WC powder fabricated on a 15CrNiMo steel. The microhardness of the Fe-WC composite coating gradually increased from 729.9HV0.2 to 1029.2HV0.2 with the increase of WC contents. The coating consisted of WC and W_2C, as well as the presence of precipitated $M_{23}C_6$, M_7C_3 and η phases. The main wear mechanisms of coatings were abrasive wear accompanied by varying degrees of adhesive wear and three-body abrasive wear. Bartkowski [27] et al. investigated the microstructure and wear resistance of Fe-based alloy reinforced by cast tungsten carbide. The coatings were composed of iron-base matrix and carbides, such as WC, $M_{23}C_6$ and $(Fe, W)_3C$ complex phases. The microhardness of the coating increased with the increase of powder feeding. The above-mentioned researches mostly focused on individual ceramic particle addition coatings, including process parameters, microstructure and properties, and cracks control.

However, there are few reports on the structure and performance of the Fe/WC-Co composite coating with cobalt bonded tungsten carbide particles to prepared metal matrix composite (MMC) coatings. In this work, FeAlC coatings with designed WC-Co addition were prepared through plasma transfer arc cladding on compacted graphite iron to improve its wear resistance. The effects of WC-Co contents on microstructures and properties of the composite coatings were investigated.

2. Experimental material and Procedure

2.1. Powder and substrate preparation

Commercial FeAlC and WC-Co powders were used as original feedstocks. They were mixed with designed mass fraction (10%, 15%, 20%, 25%) of WC-Co through a ball milling machine (ND7-

Preprints (www.preprints.org) | NOT PEER-REVIEWED | Posted: 18 December 2023 doi:10.20944/preprints202312.1334.v1

4L, Nanda Tianzun Co., Ltd Nanjing, China). The morphologies of FeAlC and WC-Co powders were shown in Figure 1 and Figure 2.

The Fe-based powder, with a mean size about 80 μm, had a near-globular shape, which was contributed to the water-atomization preparation method. WC-12Co powder, with a size about 20-80μm, had a spherical morphology, which was fabricated by agglomeration and sintering. A laser particle size analyzer (Helos-rodos, SYMPATEC GmbH., Germany) was used to characterize the particle size distribution and the average diameter of the particles (97.3 μm). Figure 3 shows their distribution. Table 1 shows the compositions of FeAlC powder. Carbon, aluminum, silicon and manganese were the main elements. Table 2 shows the compositions WC-12Co powder.

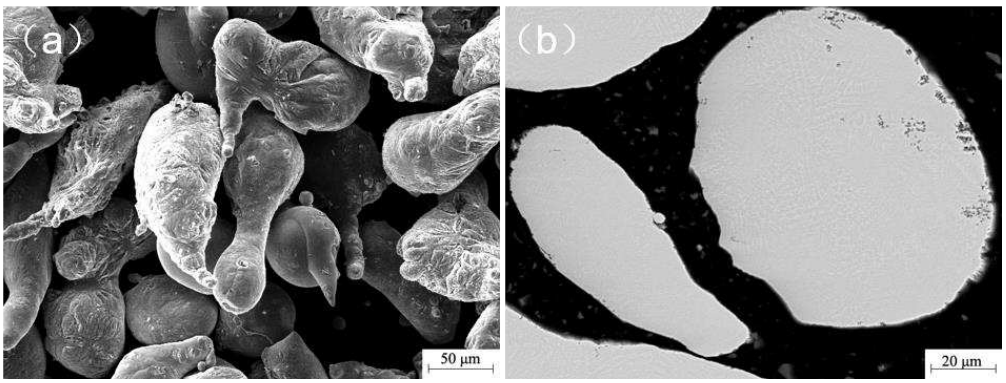

Figure 1. Microstructure of Iron-based powder:(a) global morphology, (b) Cross-sectional microstructure.

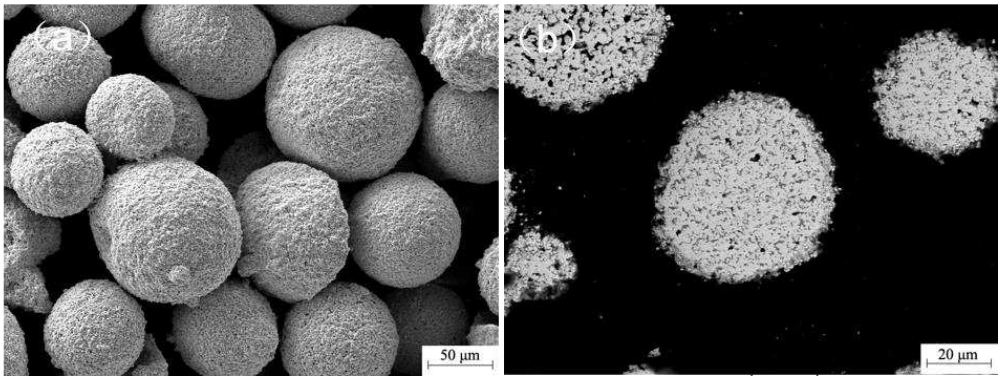

Figure 2. Microstructure of WC-12Co powder:(a) global morphology, (b) Cross-sectional microstructure.

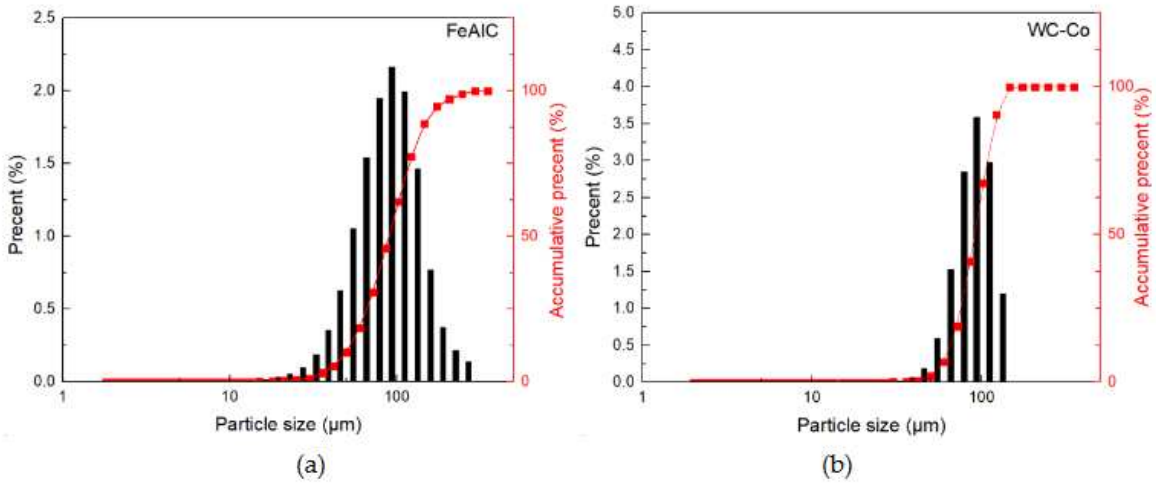

 doi:10.20944/preprints202312.1334.v1

Figure 3. Powder size distribution:(a) FeAlC powder, (b) WC-Co powder.

Figure 4 shows the morphology of the vermicular cast iron (Rut300) used as the substrate. The compacted graphite cast iron with worm-like graphite had properties between ductile iron and grey iron. Before cladding, it was necessary to remove oil and rust on the substrate to ensure a well interface combination.

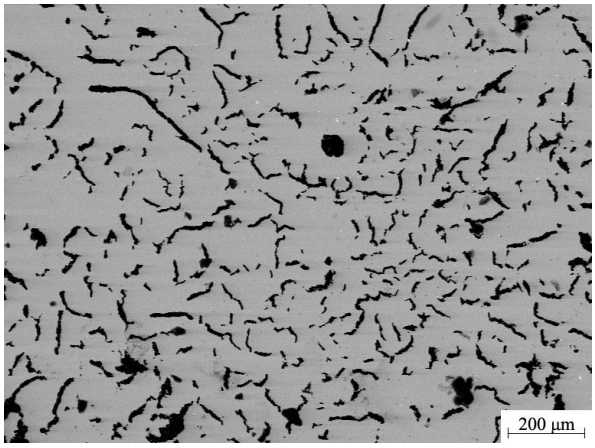

Figure 4. Microstructure of vermicular cast iron.

Table 1. Chemical composition of Fe-based powders.

Element	C	Al	Si	Mn	Fe
wt %	5.76	3.87	3.34	1.17	Bal.

Table 2. Chemical composition of WC-12Co powder.

Elements	Co	C	Fe	O	W
wt.%	11.9	5.36	0.028	0.11	Balance

2.2 Coating deposition processing

A plasma cladding system (DML-V30BD, Shanghai Duomu Co., Ltd) was applied to deposit the coating. Argon gas was used as working gas, protecting gas and powder feeding gas. The cladding parameters were listed in Table 3. During the cladding, the plasma gas flow and protective gas flow were kept on 1.5 L/min and 10 L/min. The powder feeding rated was kept at 12 rad/min. The cladding torch was manipulated with a six-axis robot at a speed of 120 mm/min. The cladding distance from the torch exit to the substrate was kept on 10 mm. The cladding currents was 65A.

Table 3. Parameters of PTA process.

Current /A	Plasma gas-flow L/min	Protective Gas flow L/min	Powder Feeding rate rad/min	Scanning velocity mm/min	Distance from Torch Exit to the Substrate mm
65	1.5	10	12	120	12

2.3 Characterization

The microstructure of the powders and coatings were characterized by scanning electron microscopy (SEM; VEGA II-XMU, TESCAN, Czech Republic). The phases of powders and coatings were analyzed by X-ray diffraction (XRD-D8, Bruker, USA) using Cu Kα radiation. The micro-

 doi:10.20944/preprints202312.1334.v1

hardness of the FeAlC-x(WC-Co) coating was measured by a Vickers micro-hardness tester (HV-5, Taiming, Shanghai, China) under a load of 200 g for a loading duration of 30 s. Wear tests were conducted on a pin-on-disk tribometer (HT-1000, Lanzhou Zhongke Kaihua Technology Development Co, Lanzhou, China). Coatings were deposited on compacted graphite cast iron with a size of φ30mm×3 mm. The counter grinding pin was made of GCr15. The test was carried out at a load of 500 g at a ring rotating speed of 150 rpm. And the sliding wear time was 30 minutes. The worn surfaces of the coatings were characterized by SEM. The wear mass loss was characterized by an electrical balance（Changzhou Xingyun Electronic Equipment Co., Ltd Changzhou, China） with an accuracy of 0.1 mg.

3. Results and discussion

3.1. Microstructure of FeAlC-x(WC-Co) coatings

Figure 5 shows the microstructure of FeAlC-10%(WC-12Co) coating. The overall coating's thickness was about 4.63 mm due to the high cladding efficiency of PTA. In the top and middle part of the cladding layer, the graphite precipitated evenly. Unmelted WC particles distributed at the bottom of the coating due to their higher density than other elements and phases. The cellular morphology showed in the top and middle of cladding layer, the planar morphology appeared at coating's bottom.

According to the theory of the rapid solidification, the temperature gradient (G) at the solid-liquid interface and the solidification rate (R) were the main factors which determined the morphology of crystal growth during the solidification of the melted alloys after plasma cladding [28]. When the plasma transfer arc interacted with the feedstocks, the molten powder could transfer the partial heat to melt the contacted surface of the substrate, resulting in metallurgical bonding. Moreover, the temperature gradient G was the largest and the solidification rate R was the smallest at the bottom of the molten pool. Therefore, the ratio G/R was nearly infinite, which in turn led to the planar growth at the bottom of the composite coatings. Meanwhile, due to the heat conduction of the cast iron matrix, the WC particles didn't get enough energy to melt so that they deposited on the bottom of the coating. Compared to Zhou's work [29], with the increase of the distance from the upper surface of the substrate, the temperature gradient G decreased and the solidification rate R increased, leading to a decrease in G/R, which would result in the growth of columnar dendrites in the coatings. While, in the FeAlC-x(WC-Co) coatings, cellular morphology formed because graphite precipitated during solidification which dissipated great heat in all directions.

Figure 5b and Figure 5c show the magnified microstructure of the middle part and bottom part. The white carbide precipitated at the graphite interface and formed a network surrounding the graphite. The carbide would be helpful to the hardness and wear resistance of the coating. Figure 5d and Figure 5e show the furtherly-magnified microstructure of the carbides in Figure 5b and Figure 5c. Table 4 shows the chemical composition of the coatings through point analysis of the elements. Point 1, the white phase, contained large amounts of W, Fe and small amounts of C. Due to a low free formation enthalpy of 38.5 kJ/mol [30], WC particles were easy to suffer from the dissolution in the molten Fe-based alloy. Babu et al. estimated that the complete dissolution time of WC was about 0.055 s in the Fe-based alloy solvent during laser cladding by using ThermoCalc software [31]. Therefore, the C and W atoms from the dissolution of WC particles could interact with Fe-based alloy formed Fe-W-C rich carbides. Point 2, the grey phase, contained Fe, W, C, Mn and Cr. It was the primary carbide as the basement to precipitated Fe-W-C rich carbides. Point 3, the dark phase, contained 86.42 wt.% carbon, which was referred as graphite. Point 4 contained mainly W, Fe and C, which was referred as WC phase mainly. Point 5 contained Fe, Al, C and Si, which were the main compositions of the original FeAlC powders although there was obvious decrease of aluminum content.

Preprints (www.preprints.org) | NOT PEER-REVIEWED | Posted: 18 December 2023 doi:10.20944/preprints202312.1334.v1

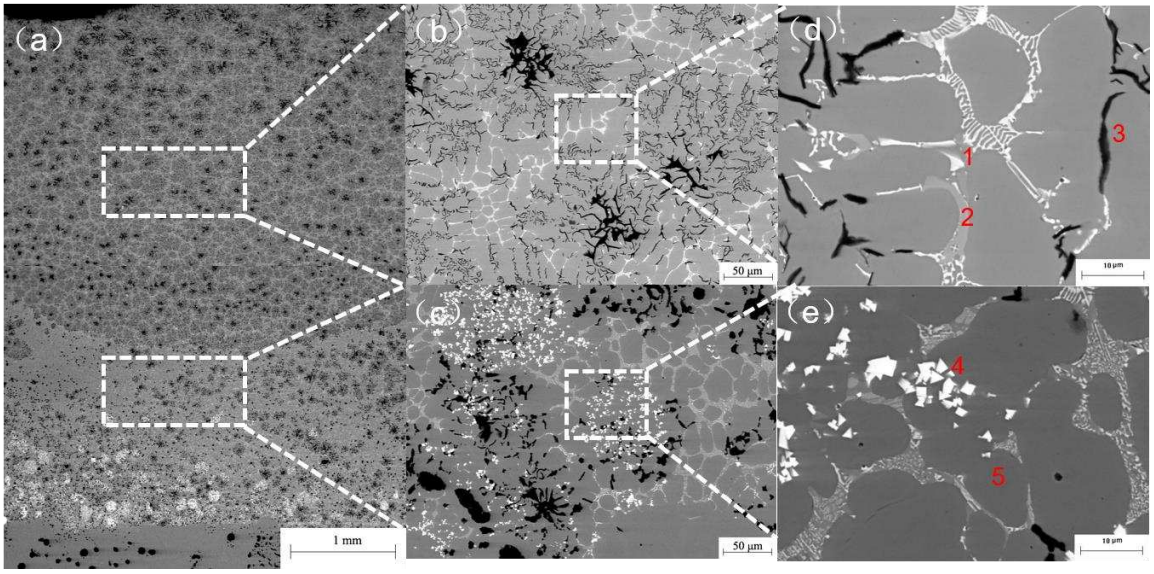

Figure 5. Cross-sectional microstructure of FeAlC-10%(WC-12Co) coating.

Figure 6 shows the cross-sectional microstructure of FeAlC-25%(WC-12Co) coating. The coating's thickness was about 4.643 mm. The coating thickness did not change significantly with the increase of the added amount of WC-Co in the same plasma cladding parameters. Figure 6b shows a magnification of position A. The precipitated carbides in the coating form a network interconnected with each other, distributed in the graphite phase gap. Figure 6c shows a magnification of position B. Large amounts of WC particles sank down at the bottom of the coating for the high density of WC in the molten pool during plasma cladding.

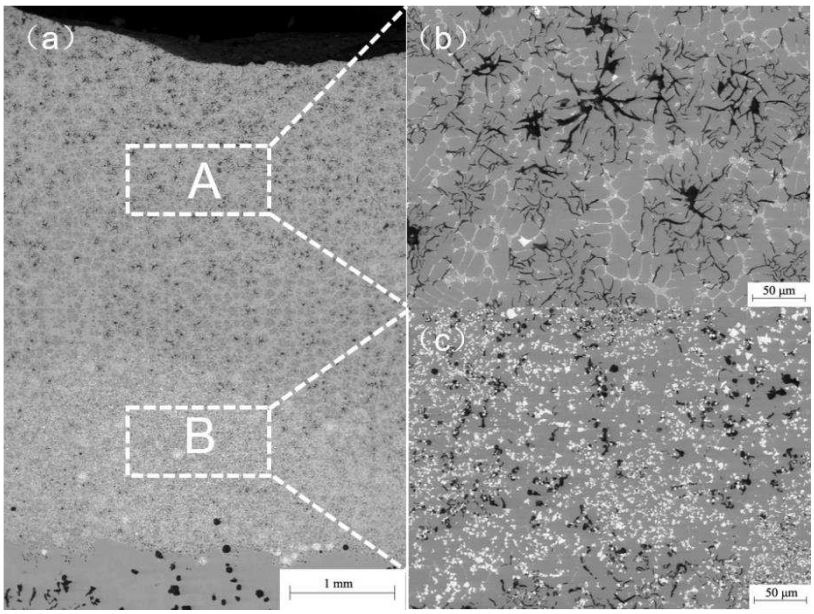

Figure 6. Cross-sectional microstructure of FeAlC-25%(WC-12Co) coating:(a) cross-sectional coating zone, (b) magnification of position A, (c) magnification of position B.

Table 4. EDS analysis of the coating/wt. %.

Element / Point	C	Fe	W	Mn	Si	Cr	Al
1	5.97	43.33	50.70	-	-	-	-

Preprints (www.preprints.org) | NOT PEER-REVIEWED | Posted: 18 December 2023 doi:10.20944/preprints202312.1334.v1

2	7.60	70.23	20.31	55.86	-	0.81	-
3	86.42	13.58	-	-	-	-	-
4	11.49	14.98	73.53	-	-	-	-
5	6.00	89.79	-	-	3.19	-	1.02

3.2. Phase compositions

Figure 7 shows X-ray diffraction patterns of the original iron-based powder and WC-12Co powder. Besides iron carbon solid solution, there were $C_{0.12}Fe_{0.79}Si_{0.09}$ and $AlFe_3C_{0.69}$ phases in the iron-based powder. There were WC and Co phases in WC-12Co powder.

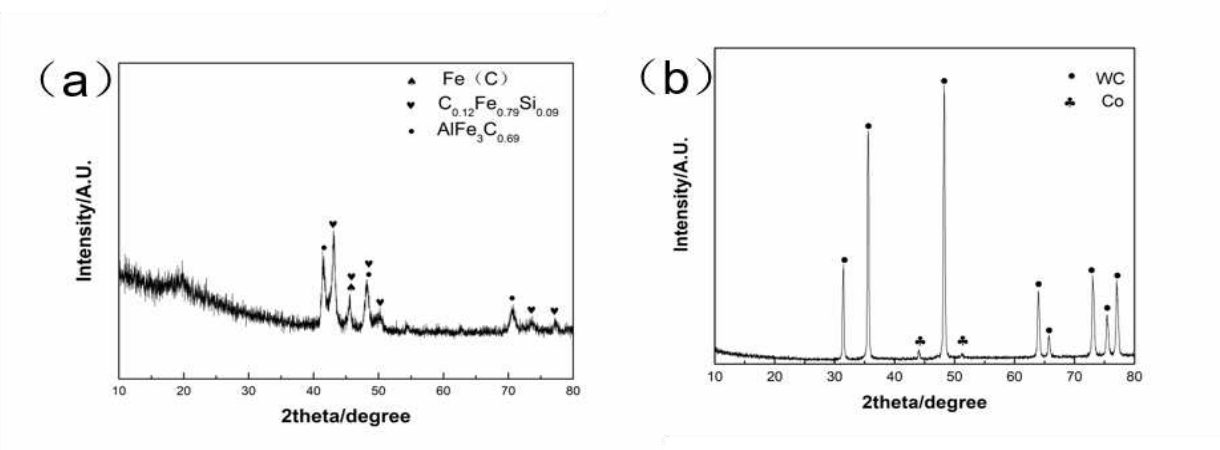

Figure 7. XRD patterns of powders:(a) Iron-based powder, (b) WC-12Co powder.

Figure 8 shows X-ray diffraction patterns of the coating's top layer and bottom layer. Austenite, martensite and WC were the mainly phases in all of the claddings due to iron-based composition and the addition of WC-12Co. Meanwhile, Fe_3W_3C formed in the coatings.During the melting of the mixed FeAlC-x(WC-Co) powders, there formed Fe_3W_3C around WC particles. In the Fe-W-C system, $3Fe+3W+C \rightarrow Fe_3W_3C$ had the lowest value of formation energy [32]. So partially Fe_3W_3C phase formed in the coating during the cladding process.

In Alireza Mostajeran's work [33], FeAl/WC composite coatings fabricated by laser cladding method contained FeAl, W_2C, Fe_3W_3C and WC phases. Presence of W_2C phase reflected the decarburization of WC during the laser cladding. Meanwhile, parts of the dissolved carbon were oxidized and departed from the melt in the form of CO and CO_2 gases, which tended to form pores inside the coating. However, in this work W_2C had not been detected. The precipitated graphite with the high capacity of heat transmission formed the Fe-rich carbides, which would inhibit the decarburization of WC.

Preprints (www.preprints.org) | NOT PEER-REVIEWED | Posted: 18 December 2023 doi:10.20944/preprints202312.1334.v1

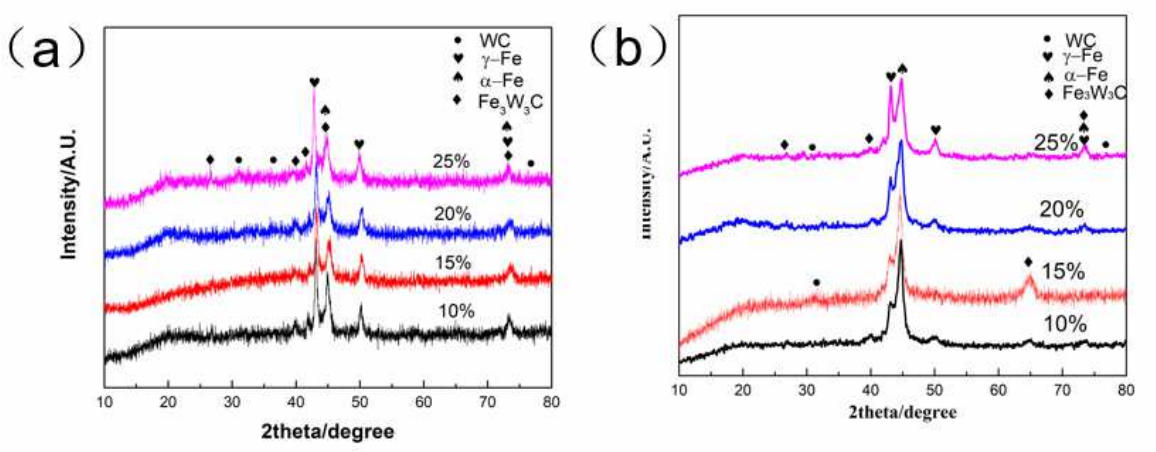

Figure 8. XRD patterns of the coatings:(a). The top and middle layer (b). The bottom layer.

3.3. Microhardness

Figure 9 shows the microhardness of FeAlC-x(WC-Co) composite coatings. With the increase of addition of WC-12Co, the microhardness of FeAlC-x(WC-Co) composite coating increased. The FeAlC-x(WC-Co) composite coating had the highest hardness of 814HV with the addition of 25wt.% WC-12Co. Zhang et al. [34] prepared Ni-Cu/WC-12Co composite coatings with 0-30 wt.% WC-12Co by laser cladding. When WC content was 0%, 10%, 20% and 30%, the microhardnesses of the coatings were 315, 318, 325 and 380HV, respectively. The microhardness of the coating increased with the increase of WC-12Co proportion. However, due to the low energy input of laser cladding in this research, the WC particle without complete melting and formed carbides. Therefore, the microhardness of the coating of was not significantly increased.

In this plasma cladding, precipitated carbides, distributing around the graphite, formed a network increased the coatings hardness. The content of WC-Co powder in the FeAlC-x(WC-Co) composite coating was controlled to a certain content, which was not very high. Otherwise, cracks would occur during the preparation of the coatings through plasma cladding, which would finally result in coating's failure.

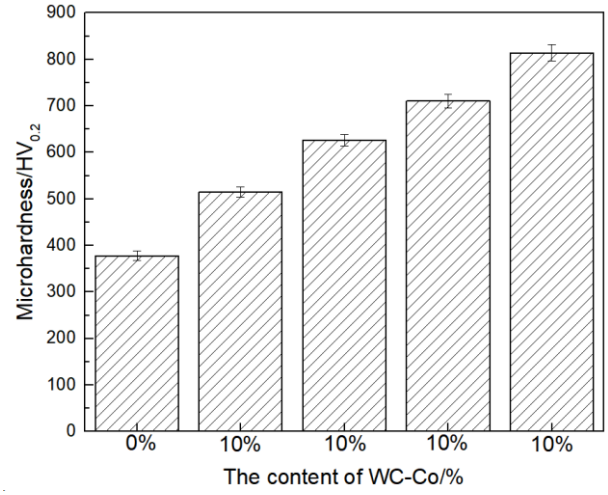

Figure 9. Microhardness of FeAlC/WC-Co composite coatings.

3.4. Tribological properties

Figure 10a shows the frictional coefficients of the compacted graphite iron substrate, the FeAlC coating and the FeAlC-x(WC-Co) composite coatings. The composite coating had the lowest frictional coefficient of about 0.5 when the content of WC-12Co powder was 20%. The frictional coefficient of the FeAlC-x(WC-Co) coatings did not increase with the increase of WC-12Co contents. The FeAlC-

 doi:10.20944/preprints202312.1334.v1

10%(WC-12Co) coating had the highest frictional coefficient of about 0.75. Graphite precipitated in the composite coatings, which would take significant antifriction effects as a solid lubricant. In our previous work [9], at the same wear condition the frictional coefficient of the compacted graphite iron substrate was 0.25, but the mass lose reached to 21.9 mg.

However, the FeAlC-20%(WC- 12Co) composite coating had the lest wear mass loss of 1.3 mg. Peng et al. [35] investigated the wear resistant of FeCoCrNi/WC coating. When WC content was 20%, 40%, 60% and 70%, the frictional coefficients of the coatings were 0.69, 0.45, 0.42 and 0.35, respectively. With the increase of WC content, the frictional coefficient of the coating decreased gradually, which indicated that the WC particles had high hardness, good wear resistance, low plastic deformation ability, limiting the increase of frictional coefficient. While, in this work, as comparison, FeAlC-20%(WC-12Co) composite coating had a mass loss 6.3 times and 16.8 times lower than FeAlC coating and compacted graphite cast iron. Therefore, FeAlC-20%(WC-12Co) had the lowest frictional coefficient and the lest wear mass loss.

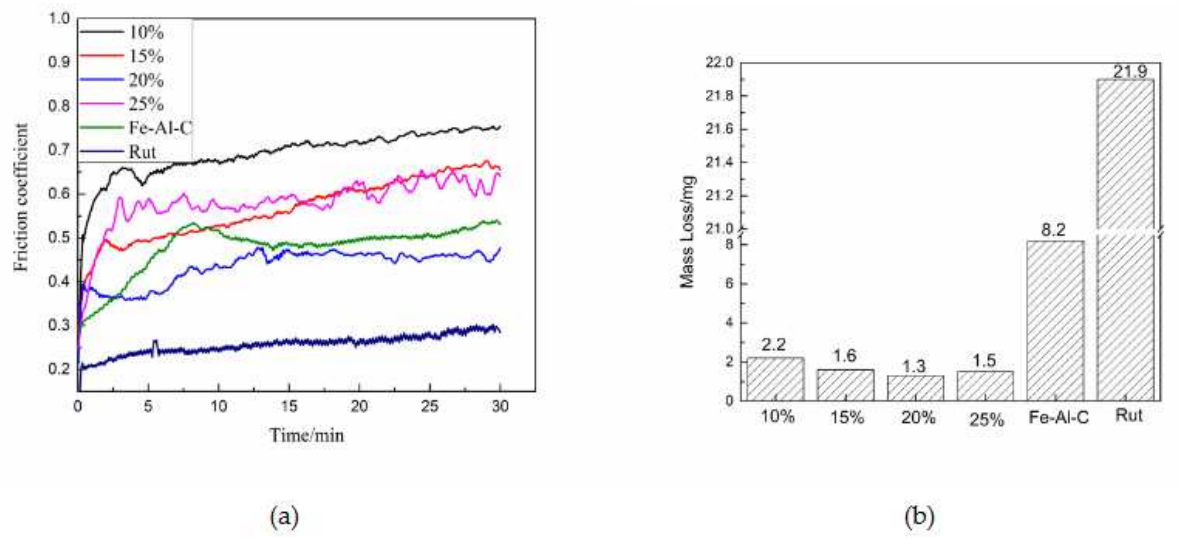

Figure 10. Friction coefficient (a) and wear mass loss (b) of FeAlC-x(WC-Co) coatings.

3.5. Worn surface and wear mechanisms

The worn surface morphologies of the FeAlC-x(WC-Co) coatings were shown in Figure 11. In the worn surface of FeAlC-x(WC-12Co) composite coating, there were obvious adhesion wear characteristics besides a large number of grooves, which reflected that the wear mechanism was a combination of adhesive wear and abrasive wear. Therefore, it would correspond to a relatively high frictional coefficient.

Preprints (www.preprints.org) | NOT PEER-REVIEWED | Posted: 18 December 2023 doi:10.20944/preprints202312.1334.v1

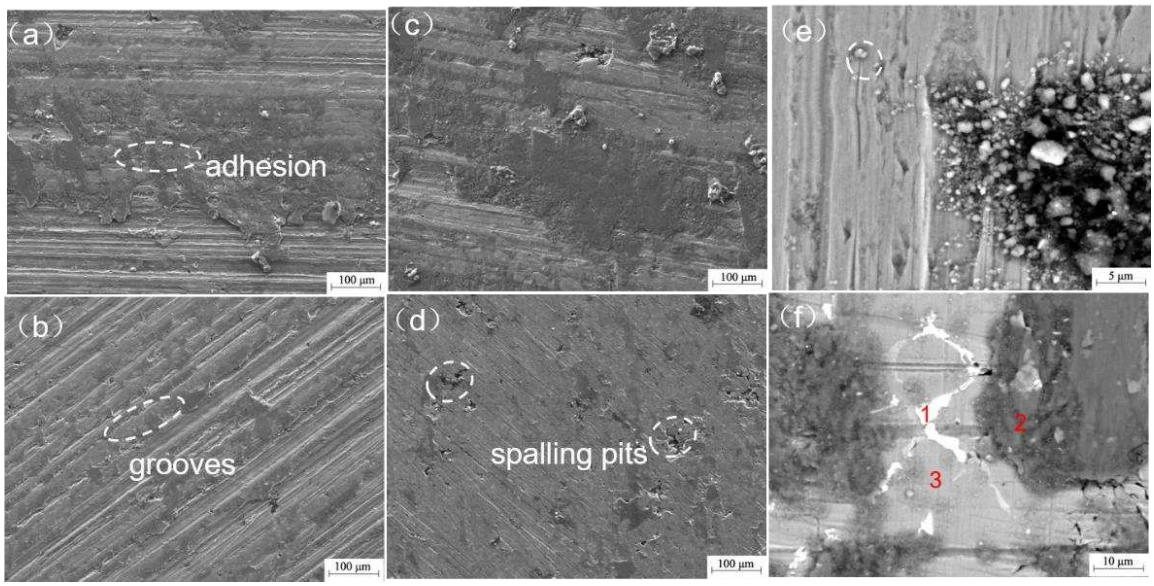

Figure 11. Worn surface morphology of FeAlC-x(WC-Co) coatings: (a)10%, (b)15%, (c)20%, (d)25%, (e)GCr15 Pin, (f) EDS analysis position of 20% coating.

When the adding of WC-12Co increased to 15%, the adhesion of the coating's worn surface began to decrease. The particles shed from the coating and teared the carbide and martensite sticked into binder phase and deformed greatly during wear test between GCr15 pin and FeAlC-15%(WC-12Co) coating, which became the main wear mechanism. Meanwhile, the pulled-out WC particles acted as abrasive particles, which were much harder than martensite [9], and plowed into martensite to form plowing in the surface of GCr15 pin as seen in Figure 11e. The FeAlC-20%(WC-12Co) coating's worn surface with light adhesive wear. As seen in Figure 11f and EDS analysis result in Table 5, there contained 34.16 wt.% carbon at point2, which was referred as graphite. Hence, the FeAlC-20%(WC-12Co) coating had the lowest frictional coefficient. Meanwhile, white carbides, containing Fe, C and W elements mainly at point 1, formed an anti-wear framework, which reduced the wear mass loss. There were spalling pits, accompanied with adhesive wear characteristics on the wear surface of FeAlC-25%(WC-12Co) coating, which inflected it experienced more serious wear than other coatings. Therefore, in terms of comprehensive evaluation, FeAlC-20%(WC-12Co) coating had best wear resistance with the lowest frictional coefficient and the lest wear mass loss.

Table 5. EDS analysis of FeAlC-20%(WC-12Co) coating after wear test.

Element / Point	C	Fe	W	O	Si	Cr	Al
1	34.16	36.21	24.3	-	4.42	0.9	-
2	34.34	44.34	-	16.87	2.22	-	2.24
3	10.56	32.31	-	56.33	0.8	-	-
4	11.49	14.98	73.53	-	-	-	-
5	6.00	89.79	-	-	3.19	-	1.02

4. Conclusions

FeAlC-x(WC-Co) composite coatings were deposited on compacted graphite cast iron through plasma transfer arc cladding. The composite coatings contained mainly γ-Fe, α-Fe, WC and Fe_3W_3C. The microhardness of the FeAlC-x(WC-Co) composite coatings had the highest hardness of 814 $HV_{0.2}$, the lowest coefficient of 0.5 and the lest wear mass loss of 1.3 mg when the addition of WC-12Co was

20 wt.%. Its wear resistance was 6.3 times and 16.8 times than FeAlC coating and the compacted graphite cast iron. It exhibited abrasive and adhesive wear mainly.

Author Contributions: Conceptualization, P.-H. G., B.-Y.C.; methodology, P.-H. G., B.-Y.C., Z.Y., Y.-C. G., and D.-M. Z.; software, P.-H. G., B.-Y.C and Q.-B. L.; validation, P.-H. G., B.-Y.C., D.-M. Z. and A. N.; formal analysis, P.-H. G., B.-Y.C and Z.Y.; investigation P.-H. G., B.-Y. C., B. Z., F. L., Q.-B. L., Y.-C. G., D.-M. Z. B.-L. W., J.-Y. G., and J.-W. L.; data curation, Z.Y.; writing—original draft preparation, B.-Y.C.; writing—review and editing, P.-H. G.; project administration, J.-P.L.; funding acquisition, P.-H. G and J.-P.L. All authors have read and agreed to the published version of the manuscript.

Funding: This work was funded by the National Natural Science Foundation of China (51771140), Foreign Experts Program of the Ministry of Science and Technology (G2022040016L), The Youth Innovation Team of Shaanxi Universities: Metal Corrosion Protection and Surface Engineering Technology, Research and application of key component materials for engines, Shaanxi Provincial Natural Science Foundation (2023-JC-YB-380), Shaanxi Provincial Key Research and Development Project (2019ZDLGY05-09), Xi'an Science and Technology Plan Project (23LLRHZDZX0019).

Institutional Review Board Statement: Not applicable.

Informed Consent Statement: Not applicable.
Data Availability Statement: Not applicable.

Conflicts of Interest: The authors declare no conflict of interest.

References

1. Z. J. Ma, D. Tao, Z. Yang, et al., The effect of vermicularity on the thermal conductivity of vermicular graphite cast iron, *Mater.Des*., 2016, 93, 418-422.
2. F. E. Mariani, G. S. Takeya, et al., Wear and corrosion resistance of Nb-V carbide layers produced in vermicular cast iron using TRD treatments, *Surf. Coat. Technol*., 2020, 397, 126050.
3. Lin, Y.; He, S.; Lai, D.; Wei, J.; Ji, Q.; Huang, J.; Pan, M. Wear Mechanism and Tool Life Prediction of High-Strength Vermicular Graphite Cast Iron Tools for High-Efficiency Cutting. *Wear.,* 2020, 454-455, 203319.
4. S. Zafar, A. K. Sharma, Development and characterisations of WC-12Co microwave clad, *Mater. Des.* 2014, 96, 241-248.
5. H. Zhou, Q. C. Guo, P. Y. Lin, et al., Influence of H13 steel unit on wear behavior of vermicular cast iron, *Appl. Surf. Sci*., 255 2008, 255, 3394-3399.
6. P. H. Gao, B. Y. Chen, S. C. Zeng, Z. Yang, et al., Effect of Vacuum Annealing on the Nickel-Based Coatings Deposited on a CGI Cast Iron through Atmospheric Plasma Spraying, *Metals.*, 2020, 10, 963-974.
7. Wang, H.; Qiu, Q.; Gee, M.; Hou, C.; Liu, X.; Song, X. Wear Resistance Enhancement of HVOF-Sprayed WC-Co Coating by Complete Densification of Starting Powder. *Mater. Des*., 2020, 191, 108586.
8. Gao, P.H.; Li, J.P.; Yang, Z.; Guo, Y.C.; Wang, Y.R. Preparation of Al/SiC Composite Coatings on Surface of Aluminum Alloy by Atmospheric Plasma Spraying. Rare. *Metal. Mat. Eng*., 2015, 44, 2396-2400.
9. Gao, P.H.; Chen, B.Y.; Wang, W.; Jia, H.; Li, J.P.; Yang, Z.; Guo, Y.C. Simultaneous increase of friction coefficient and wear resistance through HVOF sprayed WC-(nano WC-Co), *Surf. Coat. Technol.*, 2019, 363, 379.
10. Chen, B.; Gao, P.; Zhang, B.; Zhao, D.; Wang, W.; Jin, C.; Yang, Z.; Guo, Y.; Liang, M.; Li, J.; et al. Wear Properties of Iron-Based Alloy Coatings Prepared by Plasma Transfer Arc Cladding. *Coatings.*, 2022, 12, 243.
11. W. Y. Yuan, R. F. Li, Z. H. Chen, et al., A comparative study on microstructure and properties of traditional laser cladding and high-speed laser cladding of Ni45 alloy coatings, *Surf. Coat. Technol*., 2021,405, 126582.
12. D. Bartkowski, A. Mlynarczak, A. Piasecki, B. Dudziak, M. Goscianski, A. Bartkowska, Microstructure, microhardness and corrosion resistance of Stellite-6 coatings reinforced with WC particles using laser cladding, *Opt. Laser. Technol*.,2015, 68, 191–201.
13. L. Huang, J.Z. Zhou, J.L. Xu, et al., Microstructure and wear resistance of electromagnetic field assisted multi-layer laser clad Fe901 coating, *Surf. Coat. Technol.*, 2020, 395, 125876.
14. L. M. Zhang, D. B. Sun, H. Y. Yu, H. Q. Li, Characteristics of Fe-based alloy coating produced by plasma cladding process, *Mater. Sci. Eng. A*., 2007, 457, 319-324.
15. Xie, G.Z.; Song, X.L.; Zhang, D.J.; Wang, Y.P; Li, P.H. Microstructure and Corrosion Properties of Thick WC Composite Coating Formed by Plasma Cladding. *Appl. Surf. Sci*., 2010, 256, 6354-6358.
16. Zhang, L.M.; Sun, D.B.; Yu, H.Y.; Li, Y.Q. Characteristics of Fe-based alloy coating produced by plasma cladding process, *Mater. Sci. Eng. A*, 2007, 457, 319-324.

17. Gao, P.H.; Fu, R.T.; Chen, B.Y.; Zeng, S.C.; Zhang, B.; Yang, Z.; Guo, Y.C.; Liang, M.X.; Li, J.P.; Lu, Y.Q.; et al. Corrosion Resistance of CoCrFeNiMn High Entropy Alloy Coating Prepared through Plasma Transfer Arc Claddings. *Metals.*, 2021, 11, 1876.
18. Cheng; Xu; Liang; Wu Microstructure and Mechanical Characteristics of Iron-Based Coating Prepared by Plasma Transferred Arc Cladding Process. *Mater. Sci. Eng. A.*, 2008, 492, 407-412.
19. Y. H. Diao, K. M. Zhang, Microstructure and corrosion resistance of TC2 Ti alloy by laser cladding with Ti/TiC/TiB2 powders, *Appl. Surf. Sci.*, 2015, 352, 163–168.
20. G. Z. Xie, X. L. Song, D. J. Zhang, et al., Microstructure and corrosion properties of thick WC composite coating formed by plasma cladding, Appl. *Surf. Sci.*, 2010, 256, 6354-6358.
21. S. F. Zhou, X. Q. Dai, Laser induction hybrid rapid cladding of WC particles reinforced NiCrBSi composite coating, *Appl. Surf. Sci.*, 2010, 256, 4708–4714.
22. Y. B. Peng, W. Zhang, T. C Lia, et al. Effect of WC content on microstructures and mechanical properties of FeCoCrNi high-entropy alloy/WC composite coatings by plasma cladding, *Surf. Coat. Technol.*, 2020, 385, 125326.
23. K. Y. Shi, S. B. Hu, H. F. Zheng, Microstructure and fatigue properties of plasma transferred arc alloying TiC-W-Cr on gray cast iron, *Surf. Coat. Technol.*, 2011, 206, 1211-1217.
24. . Liu, Y. Wu, Y.M. Ma, W. Gao, G.Y. Yang, H. Fu, N.Y. Xi, H. Chen, High temperature wear performance of laser cladding Co06 coating on high-speed train brake disc, *Appl. Surf. Sci.*, 2019, 481, 761–766.
25. .J. Li, S.Y. Dong, S.X. Yan, X.T. Liu, B.S. Xu, Microstructure evolution during laser cladding Fe-Cr alloy coatings on ductile cast iron, *Opt Laser. Technol.*, 2018, 108, 255–264.
26. Q. Xiao, W. L. Sun, K. X. Yang, et al., Wear mechanisms and micro-evaluation on WC particles investigation of WC-Fe composite coatings fabricated by laser cladding, *Surf. Coat. Technol.*, 2021, 420, 127341.
27. D. Bartkowski, A. Bartkowska, P. Juri, Laser cladding process of Fe/WC metal matrix composite coatings on low carbon steel using Yb: YAG disk laser, *Opt. Laser Technol.*, 2021, 136, 106784.
28. Q. Y. Wang, Y. C. Xi, Y. H. Zhao, et al., Effects of laser re-melting and annealing on microstructure, mechanical property and corrosion resistance of Fe-based amorphous/ crystalline composite coating, *Mater. Charact.*, 2017, 127, 239–247.
29. S. F. Zhou, Y. B. Xu, B. Q. Liao, et al., Effect of laser remelting on microstructure and properties of WC reinforced Fe-based amorphous composite coating by laser cladding, *Opt. Laser. Technol.*, 2018, 103, 8-16.
30. C. P. Paul, H. Alemohammad, E. Toyserkani, A. Khajepour, S. Corbin, Cladding of WC-12Co on low carbon steel using a pulsed Nd:YAG laser, *Mater. Sci. Eng. A.*, 2007,464, 170–176.
31. S. S. Babu, S. A. David, R. P. Martukanitz, K. D. Parks, Toward prediction of microstructural evolution during laser surface alloying, *Metall. Mater. Trans. A.*, 2002, 33, 1189–1200.
32. Z. L. Li, H Wei, Q Shan, et al., Formation mechanism and stability of the phase in the interface of tungsten carbide particles reinforced iron matrix composites: First principles calculations and experiments, *J. Mater. Res.*, 2016, 31, 2376–2383.
33. Alireza Mostajeran, Reza Shoja-Razavi, Morteza Hadi, et al., Evaluation of mechanical properites of WC-FeAl composite coating fabricated by laser cladding method, *Int. J. Refract. Met. Hard. Mater.*, 2020, 88, 105199.
34. J. Q. Zhang, J. B. Li, Z. J. Gu, et al., Effect of WC-12Co content on wear and electrochemical corrosion properties of Ni-Cu/WC-12Co composite coatings deposited by laser cladding, *Surf. Coat. Technol.*, 2020, 393, 125807.
35. Y. B. Peng, W. Zhang, T. C. Li, et al., Microstructures and mechanical properties of FeCoCrNi high entropy alloy/WC reinforcing particles composite coatings prepared by laser cladding and plasma cladding, *Int. J. Refract. Met. Hard Mater.*, 2019, 84, 105144.